6

NUCLEAR POWER PLANT TRANSFER FUNCTIONS

E. P. Gyftopoulos and H. B. Smets
Massachusetts Institute of Technology,
Cambridge, Massachusetts

PREPRINT 53
SESSION XXI

INDUSTRIALIZING THE ATOM
CHICAGO AMPHITHEATRE
MARCH 17-21, 1958

Contributed by

American Institute of Electrical Engineers
for presentation at the

NUCLEAR ENGINEERING & SCIENCE CONFERENCE

published on behalf of
ENGINEERS
JOINT COUNCIL

by the
AMERICAN INSTITUTE OF
CHEMICAL ENGINEERS
25 West 45 Street
New York 36, New York

NUCLEAR POWER PLANT TRANSFER FUNCTIONS

by

E. P. Gyftopoulos and H. B. Smets

Introduction

The dynamic performance of a nuclear power plant is described by means of partial differential equations with respect to time and spatial variables. Therefore, a nuclear plant is a distributed parameter system.

Although this is generally recognized, the transfer functions of nuclear reactors and their associated thermal components are usually derived from lumped parameter models(1)(2)(3) and thus the partial differential equations reduce to ordinary differential equations.

In this paper an attempt is made to derive the transfer functions of a nuclear power plant from the partial differential equations with the assumption that the heat transfer coefficients are independent of temperature.

As an example, a conventional steam power plant is considered whose primary source of energy is a gas-cooled liquid metal fueled reactor (Fig. 1). However, the method of approach to the reactor itself can be applied, with only minor modifications, to any reactor with a one-phase coolant.

In the first part of the paper, the transfer functions of the reactor are derived and, in the second part, the heat exchanger and the pipes are studied.

Most of the numerical work is included in Appendices A, B and C.

1. NUCLEAR REACTOR TRANSFER FUNCTIONS

1.1 Description of the Reactor.

The gas-cooled liquid metal fueled reactor[4] consists of a graphite core through which two sets of holes are drilled. The fuel is contained in the vertical holes and the coolant passes through the horizontal ones. The core is made of twenty-three graphite elements 56 inches in length. A picture of a portion of one of them is given in Fig. 2. The core is nearly parallelepipedic and is surrounded by a graphite reflector.

The fuel is liquid bismuth containing highly enriched uranium. The vertical holes are connected by means of a manifold to a reprocessing plant. Helium is used as coolant and is blown through the reflector and then through the horizontal holes of the core at a pressure of 500 psi.

1.2 Heat Flow between the Fuel and the Coolant.

The cross section of the coolant channels is varied in such a way that the outlet coolant temperature is equal in any channel. The temperature of the moderator is approximately constant in any plane perpendicular to the coolant channels. All the heat is assumed to be released in the fuel channels and is carried away by the gas of the nearest coolant channels.

The reactor core can be divided in elementary cells like the one shown in Fig. 3. Each of those cells can be subdivided into eight subcells having the same characteristic parameters. It is reasonable to assume, with C. L. Larson[5], that no heat flows from one cell to another and from one subcell to another. Larson has also shown that the heat flow between the fuel and the gas can be computed within 6% of accuracy by considering a parallelepiped having the same cross section perpendicular to the heat flow as the subcell and a width equal to the shortest distance between the fuel and the coolant. The heat flow is therefore mostly one dimensional.

Thus the reactor can be considered as made of parallel fuel and coolant channels. Along any gas channel, heat is transferred through the graphite perpendicularly to the gas flow, from the internally heated liquid metal to the gas.

Incidentally, heat conduction in graphite in the direction of the gas channel is not appreciable, because the temperature gradient across the graphite is one hundred times larger than in the gas channel direction. Furthermore, heat convection in the fuel and heat conduction in and heat radiation from the gas are negligible.

1.3 Transfer Functions of the Reactor.

Under the assumptions of section 1.2, the effect of a variation in the gas input temperature, gas velocity and heat released in the reactor on reactivity and gas output temperature will be evaluated. Only the case of a space independent heat source will be considered here. The general case has been dealt with elsewhere by one of the authors[6].

The computations are simple but rather long, hence the derivation of only (one) transfer function will be given in detail in Appendix A.

The nomenclature of the following sections is:

b	$= \frac{hA^*}{M'c'}$	hr^{-1}
c_1	= specific heat of the moderator	BTU/lb°F
c_2	= specific heat of the fuel	BTU/lb°F
c'	= specific heat of the gas	BTU/lb°F

f_1 =	see eq. (1.5.8)	
h =	heat transfer coefficient at the gas solid interface	BTU/ft^2 hr^{o}F
k =	conductivity of the fictitious solid	BTU/ft hr^{o}F
k_1 =	conductivity of graphite	BTU/ft hr^{o}F
k_2 =	conductivity of the fuel	BTU/ft hr^{o}F
k_{eff} =	effective multiplication factor	———
ℓ =	average length of the coolant channels in the core	ft
ℓ^* =	effective neutron lifetime	hr
n =	neutron density	neutrons/ft^3
p =	resonance escape probability	———
q =	$\sqrt{\frac{s}{\alpha}}$ $q_1 = \sqrt{\frac{s}{\alpha_1}}$ $q_2 = \sqrt{\frac{s}{\alpha_2}}$	ft^{-1}
s =	complex frequency	hr^{-1}
t =	time	hr
v =	velocity of the coolant	ft/hr
x =	coordinate parallel to the coolant flow	ft
y =	coordinate parallel to the heat flow	ft
y_o, y_1, y_2	see Figs. 4 and 7	ft
A* =	effective surface of heat exchange between moderator and gas	ft^2
B^2 =	buckling	ft^{-2}
C_i =	ith delayed neutron precursor density	atoms/ft^3
M' =	mass of the gas	lb
Q =	heat source density in the fuel	BTU/ft^{3}hr
S =	1/kA* heat flow	^{o}F/ft

T =	temperature of the fictitious solid (model II)	^oF
T_1 =	temperature of the moderator	^oF
T_2 =	temperature of the fuel	^oF
T_{AV_m} =	average temperature of the moderator	^oF
T_{AV_f} =	average temperature of the fuel	^oF
α =	thermal diffusivity of the fictitious solid	ft^2/hr
α_1 =	thermal diffusivity of the moderator	ft^2/hr
α_2 =	thermal diffusivity of the fuel	ft^2/hr
β =	total fraction of delayed neutrons	——
β_1 =	fraction of delayed neutrons of i^{th} kind	——
θ =	temperature of the gas	^oF
θ_o =	inlet temperature of the gas	^oF
θ_ℓ =	outlet temperature of the gas	^oF
λ_i =	precursor decay constant (i^{th} kind)	hr^{-1}
ρ =	density of the fictitious solid (model II)	lb/ft^3
ρ_1 =	density of the moderator	lb/ft^3
ρ_2 =	density of the fuel	lb/ft^3
ρ^* =	reactivity	——
τ =	Fermi age	ft^2

Any overbarred symbol implies the Laplace transform of the increment above the steady-state value of the quantity in question.

1.4 Temperature and Power Transfer Functions - Model I.

A representative subcell of the assumed reactor is given in Fig. 4. It consists of a slab of fuel with internal distributed heat sources, insulated on one side and transmitting heat to a graphite slab on the other side. The graphite slab is cooled by the gas flow. The partial differential equations for the fuel, graphite and gas temperatures are:

$$k_2 \frac{\partial^2 T_2}{\partial y^2} + Q = \rho_2 c_2 \frac{\partial T_2}{\partial t} \qquad 1.4.1$$

$$k_1 \frac{\partial^2 T_1}{\partial y^2} = \rho_1 c_1 \frac{\partial T_1}{\partial t} \qquad 1.4.2$$

$$v \frac{\partial \theta}{\partial x} + \frac{\partial \theta}{\partial t} = b(T_1 - \theta) \qquad 1.4.3$$

The boundary conditions are:

$$y = y_2 \qquad \frac{\partial T_2}{\partial y} = 0 \qquad 1.4.4$$

$$y = y_1 \qquad k_2 \frac{\partial T_2}{\partial y} = k_1 \frac{\partial T_1}{\partial y} \qquad 1.4.5$$

$$T_2 = T_1 \qquad 1.4.6$$

$$y = 0 \qquad k_1 \frac{\partial T_1}{\partial y} = h(T_1 - \theta) \qquad 1.4.7$$

$$x = 0 \qquad \theta = \theta_o(t) \qquad 1.4.8$$

Taking the Laplace transform of equations (1.4.1) to (1.4.3) with respect to the variable t, and solving the resulting system of ordinary differential equations, it is found that the inlet temperature—outlet temperature transfer function is:

$$\frac{\overline{\theta}_\ell}{\overline{\theta}_o} = e^{-\frac{\Lambda}{\pi}\ell} \qquad 1.4.9$$

with
$$\Lambda = s\,\frac{q_2k_2}{q_1k_1}\,\sinh q_1y_1\,\sinh q_2(y_2-y_1) + (s+b)\,\frac{q_1k_1}{h}\,\sinh q_1y_1\,\cosh q_2(y_2-y_1) + s\cosh q_1y_1\,\cosh q_2(y_2-y_1) + (s+b)\,\frac{q_2k_2}{h}\,\cosh q_1y_1\,\sinh q_2(y_2-y_1) \qquad 1.4.10$$

$$\Pi = v\,\frac{q_2k_2}{q_1k_1}\,\sinh q_1y_1\,\sinh q_2(y_2-y_1) + v\,\frac{q_1k_1}{h}\,\sinh q_1y_1\,\cosh q_2(y_2-y_1) + v\cosh q_1y_1\,\cosh q_2(y_2-y_1) + v\,\frac{q_2k_2}{h}\,\cosh q_1y_1\,\sinh q_2(y_2-y_1) \qquad 1.4.11$$

The power-outlet temperature transfer function is:

$$\frac{\overline{\theta}_\ell}{\overline{Q}} = \frac{b}{hq_2}\,\frac{1-e^{-\frac{\Lambda}{\Pi}\ell}}{\Lambda}\,\sinh q_2(y_2-y_1) \qquad 1.4.12$$

Both transfer functions (1.4.9) and (1.4.12) have been plotted for all values of s along the j-axis in Figs. 5 and 6, respectively. However, they are rather cumbersome to use and, therefore, it is appropriate to examine whether it is possible to conceive a different model of heat transfer in the reactor which might lead to simpler mathematical expressions.

Various possibilities have been studied but only the one described subsequently gives results comparable to the results of model I.

1.5 Temperature and Power Transfer Functions - Model II.

A representative subcell of the approximate reactor is given in

Fig. 7. It consists of a slab of a fictitious solid whose thermodynamic properties are an appropriate average of the moderator and fuel properties of the subcell given in Fig. 4. The heat source is given as a heat flow at the fuel-graphite interface. The other side of the fictitious slab is cooled by the gas flow.

The heat balance equations for the solid and gas are:

$$\frac{\partial^2 T}{\partial y^2} = \frac{1}{\alpha}\frac{\partial T}{\partial t} \qquad 1.5.1$$

$$v\frac{\partial \theta}{\partial x} + \frac{\partial \theta}{\partial t} = b(T - \theta) \qquad 1.5.2$$

The boundary conditions are:

$$y = y_o \qquad S = \frac{Q(y_2 - y_1)}{k} = \frac{\partial T}{\partial y} \qquad 1.5.3$$

$$y = 0 \qquad k\frac{\partial T}{\partial y} = h(T - \theta) \qquad 1.5.4$$

$$x = 0 \qquad \theta = \theta_o(t) \qquad 1.5.5$$

Taking the Laplace transform of equations (1.5.1) and (1.5.2) with respect to t and solving the resulting system of ordinary differential equations, it is found (Appendix A) that the inlet temperature-outlet temperature transfer function is:

$$\frac{\bar{\theta}_\ell}{\bar{\theta}_o} = e^{-f_1 \ell} \qquad 1.5.6$$

with $$f_1 = \frac{s}{v} + \frac{b}{v}\;\frac{\frac{kq}{h}\tanh q\,y_o}{1 + \frac{kq}{h}\tanh q\,y_o} \qquad 1.5.7$$

The power-outlet temperature transfer function is:

$$\frac{\bar{\theta}_{\ell}}{\bar{Q}} = \frac{y_2 - y_1}{h \cosh q y_o} \left(\frac{s + b}{v\, f_1} - 1 \right) \left(1 - e^{-f_1 \ell} \right) \qquad 1.5.8$$

After some numerical computations given in Appendix D, the transfer functions (1.5.6) and (1.5.8) have been plotted along the j-axis in Figs. 8 and 9, respectively. Comparing those figures to Figs. 5 and 6, it is seen that model II is a good approximation of the gas-cooled liquid metal fueled reactor and since it leads to simpler mathematical expressions, it will be adopted for further calculations, unless otherwise stated.

1.6 Gas Velocity Transfer Function.

The gas-cooled reactor under consideration is designed to operate at a constant temperature rise across the reactor core. Hence, in the case of a change of the load, the gas flow and therefore the gas velocity through the system changes. Since the heat transfer coefficients depend on the gas velocity, the outlet gas temperature is a function of the gas velocity also.

Assuming small changes in gas velocity and using a perturbation method, the transfer function between gas velocity and outlet gas temperature can be derived.

The steady-state solution of equations (1.5.1) and (1.5.2) is:

$$T = \theta_o + \frac{k\,S}{h} \left(1 + \frac{bx}{v} \right) + S\,y \qquad 1.6.1$$

$$\theta = \theta_o + \frac{b\,k\,S\,x}{v\,h} \qquad 1.6.2$$

$$T - \theta = \frac{k\,S}{h} \quad \text{at } y = 0 \qquad 1.6.3$$

If a prime indicates the variation of a physical quantity for a variation of velocity, the equations for the moderator and gas temperatures are:

$$\frac{\partial^2 T'}{\partial y^2} = \frac{1}{\alpha} \frac{\partial T'}{\partial t} \qquad 1.6.4$$

$$v \frac{\partial \Theta'}{\partial x} + v' \frac{\partial \Theta}{\partial x} + \frac{\partial \Theta'}{\partial t} = b(T' - \Theta') + b'(T - \Theta) \qquad 1.6.5$$

with the boundary conditions:

$$y = y_o \qquad \frac{\partial T'}{\partial y} = 0 \qquad 1.6.6$$

$$y = 0 \qquad k \frac{\partial T'}{\partial y} = h(T' - \Theta') + h' (T - \Theta) \qquad 1.6.7$$

$$x = 0 \qquad \Theta'_o = 0 \qquad 1.6.8$$

Replacing Θ and T by their steady-state values, taking the Laplace transform of equations (1.6.4) and (1.6.5) and solving the resulting system of ordinary differential equations, it is found that the gas velocity outlet gas temperature transfer function is:

$$\frac{\bar{\Theta}'_\ell}{\bar{v}'} = \frac{k}{v^2 h f_1} \left(0.8(s - v f_1) + b\right) \left(1 - e^{-f_1 \ell}\right) S \qquad 1.6.9$$

In the derivation, it is assumed that the parameters b and h vary like the 0.8 power of the gas velocity.

A plot of equation (1.6.9) along $s = j\omega$ is given in Fig. 10.

1.7 <u>Temperature Dependence of Reactivity</u>.

The reactivity depends on the average moderator and fuel temperatures. Any variation of gas inlet temperature, heat rate released in the fuel or gas velocity affect the reactor temperatures.

The variation of reactivity is given by:

$$\delta\rho^* = \left(\frac{\partial \rho^*}{\partial T_{AV_m}}\right) \delta T_{AV_m} + \left(\frac{\partial \rho^*}{\partial T_{AV_f}}\right) \delta T_{AV_f} \qquad 1.7.1$$

The partial derivatives of reactivity with respect to T_{AV_m} and T_{AV_f} can be easily found.[7]

The average temperatures are derived by integrating the temperatures for one cell and weighting the average cell temperature by the square of the neutron flux in a first-order approximation and further integrating throughout the cubic core. However, in the present case, the heat rate has been assumed constant and therefore the average temperature of one cell is adequate.

1.8 Moderator Average Temperature and Transfer Functions.

The temperature of the fictitious solid is a good approximation to the moderator temperature and it will be used to evaluate the average temperature of the latter.

The temperature of the fictitious solid is a solution of equations (1.5.1) and (1.5.2) and is equal to:

$$\overline{T} = A' \cosh q\, y + B' \sinh q\, y \qquad 1.8.1$$

where A', B' are constants determined from the boundary conditions (1.5.3) to (1.5.5).

Assuming a small perturbation in the input temperature, the power level and the gas velocity, and after some algebra, the average temperature of the moderator is found to be:

$$\overline{T}_{AV_m} = \frac{\tanh qy_o}{f_1 \ell q y_o \left(1+\frac{kq}{h}\tanh qy_o\right)}\left(1 - e^{-f_1 \ell}\right)\overline{\theta}_o + \\ + \left\{\frac{\tanh qy_o}{hqy_o\left(1+\frac{kq}{h}\tanh qy_o\right)\cosh qy_o}\left[\frac{1-e^{-f_1\ell}}{f_1\ell} + \frac{s+b}{vf_1}\left(1-\frac{1-e^{-f_1\ell}}{f_1\ell}\right)\right] + \frac{\cosh qy_o - 1}{kq^2 y_o \cosh qy_o}\right\}(y_2-y_1) \\ + \frac{k\tanh qy_o}{hqy_o v}\;\frac{\frac{1-e^{-f_1\ell}}{f_1\ell}\left(0.8 - \frac{0.8s+b}{vf_1}\right) + \frac{0.8s+b}{vf_1}}{1+\frac{kq}{h}\tanh qy_o}\;\overline{v}' \qquad 1.8.2$$

A plot of the transfer functions associated with equation (1.8.2) is given in Figs. 11, 12 and 13.

1.9 Fuel Average Temperature and Transfer Functions

The computations for the fuel average temperature are similar to the ones for the moderator. However, in this case, model I is used, since model II does not take properly into account the fuel volume.

Solving the system of equations (1.4.1) to (1.4.3) with the proper boundary conditions, it is found that:

$$\overline{T}_{AV_f} = \frac{v}{\ell(y_2-y_1)}\left[\frac{1-e^{-\frac{\Lambda}{n}\ell}}{q_2\Lambda} \sinh q_2(y_2-y_1)\right]\overline{\theta}_o +$$

$$+\left[\frac{vb}{\ell q_2^2 (y_2-y_1)} \frac{\left(\ell\frac{\Lambda}{n} - 1 + e^{-\frac{\Lambda}{n}\ell}\right)}{\Lambda^2 h} \sinh^2 q_2(y_2-y_1) + \frac{\alpha_2}{k_2 s}\right]\overline{Q} +$$

$$+ \frac{Q(y_2-y_1)}{h\,n} \frac{\sinh q_2(y_2-y_1)}{q_2(y_2-y_1)}\left[0.8\,\frac{1-e^{-\frac{\Lambda}{n}\ell}}{\Lambda\ell}\,n + \frac{0.8s+b}{v\Lambda}\,n\left(1-\frac{1-e^{-\frac{\Lambda}{n}\ell}}{\ell\Lambda}\,n\right)\right]\overline{v}'$$

1.10 Neutron Kinetics Transfer Function.

The power released in a nuclear reactor is proportional to the neutron flux which can be computed from the neutron kinetics equations.

$$\frac{dn}{dt} = \left[k_{eff}\,(1-\beta) - 1\right]\frac{n}{\ell^*} + e^{-B^2\tau} \sum_i \lambda_i C_i \qquad 1.10.1$$

$$\frac{dC_i}{dt} = \beta_i \frac{k_{eff}}{e^{-B^2\tau}} \frac{n}{\ell^*} - \lambda_i C_i \qquad 1.10.2$$

For small variations of k_{eff} around the steady-state value the neutron kinetics equations can be linearized and the following transfer function is found[8]:

$$\frac{\overline{Q}}{\overline{k}} = Q \frac{1 - s \sum_i \frac{\beta_i}{s + \lambda_i}}{s\left(\ell + \sum_i \frac{\beta_i}{s + \lambda_i}\right)} \qquad 1.10.3$$

1.11 Reactor Block Diagram.

All the transfer functions derived in the previous treatment have been assembled together in Fig. 14 to give a block diagram representation of the reactor.

The reactor is considered as having two inputs, the gas input temperature and velocity, and one output, the gas output temperature. Inside the reactor, various feedback loops relate power and reactivity to temperature.

2. HEAT EXCHANGER TRANSFER FUNCTIONS

2.1 Heat Exchanger Description.

From the outlet of the reactor, the hot gas is piped to the heat exchanger where heat is transferred to the secondary coolant loop. The heat exchanger is of the counterflow type and consists of an economizer, a boiler and a superheater. The secondary coolant is water.

Each of the three components of the heat exchanger may be visualized as consisting of a single tube containing the secondary coolant in the proper phase and surrounded by helium gas, which in turn is contained in a concentric shell (Fig.15).

2.2 Transfer Functions of the Heat Exchanger.

The transfer functions between the incoming fluid temperatures and the outgoing fluid temperatures will be derived for the superheater and the boiler. The transfer functions of the economizer are similar to the ones of the superheater since in both cases it is assumed that the secondary coolant is in the liquid or vapor phase respectively.

The assumptions behind the derivation of the transfer functions are:

(a) The turbulence is very high in both fluids.

(b) The heat conduction along the axial direction of the tube and the shell is zero.

(c) The heat conductivity of the tube and the shell along the radius is infinite.

(d) The heat losses to the surrounding are zero.

(e) The heat transfer coefficients are constant.

The nomenclature of the following sections is:

$a_1 = \dfrac{h_1 A_1}{M_1 c_1}$ $\qquad hr^{-1}$

$a_2 = \frac{h_2 A_2}{M_2 c_2}$ hr^{-1}

$a_3 = \frac{h_3 A_3}{M_3 c_3}$ hr^{-1}

$b_1 = \frac{h_1 A_1}{M_3 c_3}$ hr^{-1}

$b_2 = \frac{h_2 A_2}{M_3 c_3}$ hr^{-1}

$b_3 = \frac{h_3 A_3}{M_4 c_4}$ hr^{-1}

c_1 = specific heat of water BTU/lb °F

c_2 = specific heat of helium BTU/lb °F

c_3 = specific heat of the tube BTU/lb °F

c_4 = specific heat of the shell BTU/lb °F

$f_1 = \frac{1}{v_1}\left[s + \frac{a_1(s+b_2)}{s+b_1+b_2}\right]$ $\quad f_2 = \frac{1}{v_2}\left[s + \frac{a_2(s+b_1)}{s+b_1+b_2} + \frac{a_3 s}{s+b_3}\right]$ ft^{-1}

$f_3 = \frac{1}{v_1}\ \frac{a_1 b_2}{s+b_1+b_2}$ $\quad f_4 = \frac{1}{v_2}\ \frac{a_2 b_1}{s+b_1+b_2}$ ft^{-1}

$f_5 = s + \frac{s+b_1}{s+b_1+b_2}\, a_2 + \frac{s}{s+b_3}\, a_3$ ft^{-1}

h_1 = heat transfer coefficient on the water side BTU/ft^2 hr °F

h_2 = heat transfer coefficient on the helium side BTU/ft^2 hr °F

h_3 = heat transfer coefficient on the shell side BTU/ft^2 hr °F

ℓ = superheater length ℓ' = boiler length ft

s = complex frequency hr^{-1}

t = time hr

v_1 = water velocity ft/hr

v_2	=	helium velocity	ft/hr
x	=	running length along the heat exchanger	ft
A_1	=	surface of tube on the water side	ft^2
A_2	=	surface of tube on the helium side	ft^2
A_3	=	surface of the shell	ft^2
F	=	fluid flow through the mixing volume	ft^3/hr
M_1	=	mass of water inside the tubes	lb
M_2	=	mass of helium inside the heat exchanger	lb
M_3	=	mass of the tube	lb
M_4	=	mass of the shell	lb
V	=	mixing volume	ft^3
T	=	transport time between the reactor and the heat exchanger	hr
α	=	$\frac{1}{2}(f_2 - f_1)$	ft^{-1}
β	=	$\frac{1}{2}\sqrt{(f_2 + f_1)^2 - 4f_3f_4}$	ft^{-1}
λ	=	see equation (2.3.9)	——
θ_1	=	water temperature	^oF
θ_{10}	=	inlet water temperature	^oF
$\theta_{1\ell}$	=	outlet water temperature	^oF
θ_2	=	helium temperature	^oF
θ_{20}	=	outlet helium temperature	^oF
$\theta_{2\ell}$	=	inlet helium temperature	^oF

θ_{in} = temperature of the fluid before mixing ^{o}F

θ_{out} = temperature of the fluid after mixing ^{o}F

ϕ_1 = tube temperature ^{o}F

ϕ_3 = shell temperature ^{o}F

Any overbarred symbol implies the Laplace transform of the increment above the steady-state value of the quantity in question.

2.3 Superheater Transfer Functions.

In the superheater section of the heat exchanger the secondary coolant is in the vapor phase. A heat balance in an elementary volume of the superheater results in the following equations for the steam, the internal tube, the helium gas and the external shell respectively (Fig.15):

$$\frac{\partial \theta_1}{\partial t} + v_1 \frac{\partial \theta_1}{\partial x} = a_1 (\phi_1 - \theta_1) \qquad 2.3.1$$

$$\frac{\partial \phi_1}{\partial t} = b_1(\theta_1 - \phi_1) + b_2(\theta_2 - \phi_1) \qquad 2.3.2$$

$$\frac{\partial \theta_2}{\partial t} - v_2 \frac{\partial \theta_2}{\partial x} = a_2(\phi_1 - \theta_2) + a_3 (\phi_3 - \theta_2) \qquad 2.3.3$$

$$\frac{\partial \phi_3}{\partial t} = b_3(\theta_2 - \phi_3) \qquad 2.3.4$$

The boundary conditions are:

$$x = 0 \qquad \theta_1 = \theta_{1\ell}, \qquad 2.3.5$$

$$x = \ell \qquad \theta_2 = \theta_{2\ell} \qquad 2.3.6$$

The solution of the system (2.3.1) to (2.3.4) in terms of the complex frequency s, is found to be:

$$\bar{\theta}_1 = \bar{\theta}_{10} \frac{e^{\alpha x} \sinh[\beta(\ell - x) + \lambda]}{\sinh(\beta\ell + \lambda)} + \bar{\theta}_{2\ell} \sqrt{\frac{f_3}{f_4}} \frac{e^{\alpha(x-\ell)} \sinh \beta x}{\sinh(\beta\ell + \lambda)} \quad 2.3.7$$

$$\bar{\theta}_2 = \bar{\theta}_{10} \sqrt{\frac{f_4}{f_3}} \frac{e^{\alpha x} \sinh \beta(\ell - x)}{\sinh(\beta\ell + \lambda)} + \bar{\theta}_{2\ell} e^{\alpha(x-\ell)} \frac{\sinh(\beta x + \lambda)}{\sinh(\beta\ell + \lambda)} \quad 2.3.8$$

where λ is defined by the equation:

$$\sinh_{\lambda} = \frac{\beta}{\sqrt{f_3 f_4}} \quad 2.3.9$$

The transfer functions relating gas and steam inputs to gas and steam outputs are obtained by replacing x by 0 or ℓ in accordance with the case. They are given explicitly in Fig. 16 and have been plotted for $s = j\omega$ in Figs. 17a and b.

2.4 Boiler Transfer Function .

In the boiler section of the heat exchanger the secondary coolant is in the saturated vapor phase and its temperature is constant when the steam pressure is constant. The heat balance equations for the internal tube, the helium gas and the shell are the same as equations (2.3.2) to (2.3.4) with θ_1 constant.

The boundary conditions are:

$$x = 0 \qquad \theta_2 = \theta_{2\ell'}(t) \quad 2.4.1$$

The solution of this system of equations in terms of the complex frequency gives the gas transfer function as:

$$\bar{\theta}_{2\ell''} = \bar{\theta}_{2\ell'} \quad e^{-f_5 \frac{\ell'}{v_2}} \quad 2.4.2$$

2.5 Fluid Flow Transfer Functions.

The effect of flow variations of the fluids going through the heat exchanger has been studied by a perturbation method(6) but the formulae obtained are complicated and long and they are omitted from this presentation.

2.6 Steam Drum, Mixing Volumes and Pipe Transfer Functions.

Mixing in the steam drum, or at any mixing volume at the inputs or outputs of the reactor or the heat exchanger, introduces a single lag transfer function of the form:

$$\frac{\bar{\theta}_{out}}{\bar{\theta}_{in}} = \frac{1}{1 + \frac{V}{F} s} \qquad 2.6.1$$

Pipe connections have a pure time delay associated with them. The transfer function of a pipe is e^{-sT}.

2.7 Heat Exchanger Block Diagram.

The time behavior of the heat exchanger under inlet temperature variation is a problem of moving boundary conditions. For instance, as the inlet water temperature increases the economizer tube length is decreased, boiling starts earlier and hence the superheater tube length is increased.

A first approximation to this can be obtained by considering the lengths of the components of the heat exchanger constant and by assembling in a block diagram (Fig. 18) the transfer functions of the superheater, the boiler, the steam drum and the ones of the economizer which are similar to the transfer functions of the superheater. As a perturbation in the vapor inlet temperature takes time to propagate through the boiler, a pure delay transfer function has also been included. The approximation is good in a quasi-steady state when the gradient of the secondary coolant temperature in the economizer and the superheater are equal and the boiling tube length is constant (Fig. 19 a, b, c).

3. STEAM PLANT

The steam from the heat exchanger is fed into a turbine which is coupled to an alternator. The entire steam plant is conventional in every respect.

The derivation of the steam plant transfer functions has been dealt with for many years. The turbine-alternator transfer functions have been given by M. Riaz(8), M. Mesarovic and I. Obradovic(9) and W. A. Heffron and R. A. Phillips(10) Transfer functions of d-c motors and generators as well as pumps can be found in many textbooks. The condenser is the only distributed parameter system and it can be handled like the heat exchanger with one of the fluids at constant temperature. Equation (2.4.2) may be used.

4. POWER PLANT BLOCK DIAGRAM

The block diagrams of the reactor (Fig. 14) and the heat exchanger (Fig. 18) as well as the block diagrams of the mixing volumes and pipes are assembled in Fig. 20, which is a block diagram of the power plant.

5. CONCLUSION

The transfer functions of the main components of a nuclear power plant, i.e., the reactor, the heat exchanger and the condenser have been derived. Those components are distributed parameter systems and the transfer functions are obtained by integration of a set of partial differential equations. The method is simple and straightforward when the Laplace transform technique is used.

The obtained transfer functions can be approximated for low frequencies by rational functions of the complex frequency s and exponentials of s. Thus they can be represented by electric networks and delay lines.

As a final word, it is hoped that this work will be useful for the analog study of a reactor as it gives a better representation of the reactor and its associated power plant.

ACKNOWLEDGMENT

The authors are greatly indebted to the Nuclear Power Group of the Raytheon Manufacturing Company for giving data on the gas-cooled liquid metal fueled reactor.

One of the authors thanks also the Belgian American Educational Foundation which granted him a C.R.B. Graduate Fellowship.

REFERENCES

1. J. C. Moise, "Application of Analog Computing Techniques to Reactor Dynamics," Chem. Eng. Progr. Symp., 12, pp.96-106 (1954).

2. R. G. Olson, D. J. Ritchie, "Transient Temperature Simulation of Reactor Primary Loop," APDA 111, 1956.

3. R. G. Olson, "Dynamic Simulation of a Fast Reactor," Nucleonics, 15, 5, pp. 76-9 (1957).

4. Liquid Metal Fuel-Gas Cooled Reactor. A nuclear plant for competitive power. Raytheon Manufacturing Company.

5. C. L. Larson, "Temperature Distribution between Mutually Perpendicular Fuel and Coolant Channels of a Nuclear Reactor." Report of the Research Division, Raytheon Manufacturing Company, Waltham (to be published).

6. H. B. Smets, "Nuclear Power Plant Transfer Functions," S.M. Thesis, Nuclear Engineering Department, Massachusetts Institute of Technology, 1957.

7. S. Glasstone, PRINCIPLES OF NUCLEAR REACTOR ENGINEERING, Van Nostrand, New York (1955).

8. M. Riaz, "Analogue Computer Representation of Synchronous Generators in Voltage Regulation Studies," AIEE Trans. 75, III, pp. 1178-84 (1956).

9. M. Mesarovic, I. Obradovic, "Influence of a Supplied Power System on the Frequency Control," C.I.G.R.E. 1956, p. 321.

10. W. A. Heffron, R. A. Phillips, "Effects of a Modern Amplidyne Voltage Regulator on Underexcited Operation of Large Turbine Generators," AIEE Trans., 71, III, pp. 692-7 (1952).

Appendix A. DERIVATION OF THE POWER AND TEMPERATURE TRANSFER FUNCTIONS.

In this appendix, the derivation of equations (1.5.6) and (1.5.8) are given. The Laplace transform of equations (1.5.1) to (1.5.3) and (1.5.5) are:

$$\frac{d^2 \bar{T}}{dy^2} = \frac{s}{\alpha} \bar{T} \qquad \text{A1}$$

$$v \frac{d\bar{\theta}}{dx} + s\bar{\theta} = b(\bar{T} - \bar{\theta}) \qquad \text{A2}$$

$$y = y_o \qquad \bar{S} = \frac{d\bar{T}}{dy} \qquad \text{A3}$$

$$x = 0 \qquad \bar{\theta} = \bar{\theta}_o \qquad \text{A4}$$

The solution of (A1) is:

$$\bar{T} = A \cosh qy + B \sinh qy \qquad \text{A5}$$

Equation (A5) is used in (1.5.4) which reduces to:

$$\bar{\theta} = A - \frac{kBq}{h} \qquad \text{A6}$$

Using (A5) and (A6) in (A2) and (A3), it is found that:

$$v \frac{dA}{dx} - \frac{kq}{h} v \frac{dB}{dx} + sA - s \frac{kqB}{h} = b \frac{k}{h} Bq \qquad \text{A7}$$

$$\bar{S} = qA \sinh qy_o + qB \cosh qy_o \qquad \text{A8}$$

Eliminating B between (A7) and (A8), it is found that:

$$\frac{dA}{dx} + f_1 A = f_2 \bar{S} \qquad \text{A9}$$

with
$$f_1 = \frac{s}{v} + \frac{b}{v} \times \frac{\frac{kq}{h} \tanh qy_o}{1 + \frac{kq}{h} \tanh qy_o} \qquad \text{A10}$$

$$f_2 = \frac{k(s + b)}{vh \cosh qy_o} \times \frac{1}{1 + \frac{kq}{h} \tanh qy_o} \qquad \text{A11}$$

The solution of (A9) is:

$$A = e^{-f_1 x} \left[c + \bar{S}\, f_2 \; \frac{e^{f_1 x} - 1}{f_1} \right] \qquad \text{A12}$$

where c is a constant which will be determined. Eliminating B between (A6) and (A8), $\bar{\theta}$ is given by

$$\bar{\theta} \; = \; A \left(1 + \frac{kq}{h} \; \tanh qy_o\right) \; - \frac{k}{h} \; \frac{\bar{S}}{\cosh \, qy_o} \qquad \text{A13}$$

Replacing A by its value (A12), the gas temperature is:

$$\bar{\theta} = \bar{\theta}_o \; e^{-f_1 x} \; + \; \bar{S} \; \left[\frac{k}{h \cosh \, qy_o} \left(\frac{s+b}{vf_1} - 1 \right) \left(1 - e^{-f_1 x} \right) \right] \qquad \text{A14}$$

where c has been chosen such that $\bar{\theta} = \bar{\theta}_o$ at $x = 0$.

Appendix B. NUMERICAL COMPUTATIONS OF THE TEMPERATURE AND POWER TRANSFER FUNCTIONS.

In this appendix, the computations of the transfer functions for the gas-cooled liquid metal fueled reactor are given. The values of the parameters are given in Table I. For the numerical computation, Kennelly's[1] Tables of Complex Hyperbolic Functions are useful.

Asymptotic behavior.

(1) Temperature transfer functions:

For low frequencies

Model I: $$\frac{\bar{\theta}_\ell}{\bar{\theta}_o} = e^{-j\frac{\omega \ell}{v}}\left[1 + b\left(\frac{k_2}{\alpha_2}\times\frac{y_2-y_1}{h} + \frac{k_1}{\alpha_1}\;\frac{y_1}{h}\right)\right] \simeq 1 \qquad \text{B1}$$

Model II: $$\frac{\bar{\theta}_\ell}{\bar{\theta}_o} = e^{-j\frac{\omega \ell}{v}}\left(1 + b\frac{k}{h}\;\frac{y_o}{\alpha}\right) \simeq 1 \qquad \text{B2}$$

In order to have a good agreement of model II with model I at low frequencies, the average value of the parameters of model II are taken such that

$$\frac{k_1 y_o}{\alpha} = k_1\;\frac{y_1}{\alpha_1} + \frac{k_2(y_2-y_1)}{\alpha_2} \qquad \text{B3}$$

and $$\frac{1}{\alpha} = \left(\frac{\rho c}{k}\right)_{av} = \frac{M_1\frac{1}{\alpha_1} + M_2\frac{1}{\alpha_2}}{M_1 + M_2} \qquad \text{B4}$$

where M_1 = mass of moderator

M_2 = mass of fuel

For high frequencies

Models I and II: $$\frac{\bar{\theta}_\ell}{\bar{\theta}_o} = e^{\frac{-b\ell}{v}}\;e^{-j\frac{\omega \ell}{v}} \qquad \text{B5}$$

(2) Power transfer functions:

For low frequencies

<u>Models I and II:</u> $$\frac{\bar{\Theta}_\ell}{\bar{Q}} = (y_2 - y_1)\frac{b\ell}{vh} \qquad \text{B6}$$

For high frequencies

<u>Models I and II:</u> $$\frac{\bar{\Theta}_\ell}{\bar{Q}} = 0 \qquad \text{B7}$$

TABLE I

Data for the Computation of the Temperature and Power Transfer Functions

b	=	$\frac{hA}{M'c'}$	=	$226{,}000\ hr^{-1}$
h	=	heat transfer coefficient	=	$1{,}100\ BTU/ft^2\ hr\ ^oF$
k_1	=	conductivity of graphite	=	$36.2\ BTU/hr\ ft\ ^oF$
ℓ	=	average length of the gas channels	=	3 ft
v	=	gas velocity in the channels	=	1,710,000 ft/hr
y_o	=	weighted moderator thickness	=	2.217×10^{-2} ft
$y_2 - y_1$	=	graphite thickness	=	1.785×10^{-2} ft
α	=	average thermal diffusivity	=	$0.45\ ft^2/hr$

Approximation

As the desired transfer functions may be used for an analogue study of the reactor, they are hereafter approximated by electric lumped networks and delay lines. The equivalent networks that are given have transfer functions that satisfy the following requirements.

They give the same behavior at zero and infinite frequencies when compared to the exact transfer functions.

They fit the exact transfer functions on a frequency range where the attenuation varies from 0 to 20 db.

Since the distributed parameter systems are not phase minimum, the standard methods of approximation in the frequency domain do not apply. In this case, the type of approximate transfer function is chosen by inspection of the s = jω plot of the approximated transfer function. The parameters of the approximate transfer function are adjusted by trial and error.

The approximate transfer functions for models I and II are:

$$\frac{\bar{\theta}_\ell}{\bar{\theta}_o} = \left[e^{-\frac{b\ell}{v}} + \frac{\left(1 - e^{-\frac{b\ell}{v}}\right)\left(1 + \frac{s}{782}\right)}{\left(1 + \frac{s}{2500}\right)\left(1 + \frac{s}{312}\right)} \right] \times e^{-\frac{s\ell}{v}} \quad \text{(Figs. 5 and 8)} \qquad \text{B8}$$

$$\frac{\bar{\theta}_\ell}{\bar{Q}} \propto \frac{1}{1 + 2.82 \times 10^{-3}\, s} \times \frac{1 - 1.74 \times 10^{-4}\, s}{1 + 1.74 \times 10^{-4}\, s} \quad \text{(Fig. 6)} \qquad \text{B9}$$

$$\frac{\bar{\theta}_\ell}{\bar{Q}} \propto \frac{1}{1 + 2.48 \times 10^{-3}\, s} \times \frac{1 - 1.305 \times 10^{-4}\, s}{1 + 1.305 \times 10^{-4}\, s} \quad \text{(Fig. 9)} \qquad \text{B10}$$

Reference

1. A. E. Kennelly, "Tables of the Complex Hyperbolic Functions," Harvard University Press, 1914.

   A. E. Kennelly, "Chart Atlas of Complex Hyperbolic Circular Functions," Harvard University Press, 1914.

Appendix C. TRANSFER FUNCTIONS OF THE HEAT EXCHANGER.

In this appendix, the computation of the transfer functions of the heat exchanger are given. The following values for the parameters have been chosen.

$$a_1 = 300$$
$$v_1 = 2000 \text{ ft/hr}$$
$$a_2 = 250$$
$$v_2 = 90{,}000 \text{ ft/hr}$$

They are good estimates of the parameters of the high pressure steam superheater at Calder Hall. The tube and shell heat capacitieshave been neglected. The transfer functions $\frac{\bar{\theta}_{1\ell}}{\bar{\theta}_{2\ell}}$ and $\frac{\bar{\theta}_{2\ell'}}{\bar{\theta}_{1\ell'}}$ are proportional to each other and have been plotted in Fig. 17a after normalization to 1 for s = 0. At s = ∞, they are equal to zero. The functions $\frac{\bar{\theta}_{1\ell}}{\bar{\theta}_{1\ell'}}$ and $\frac{\bar{\theta}_{2\ell'}}{\bar{\theta}_{2\ell}}$ have nearly circular plots (Fig. 17b).

An approximation to the transfer function $\frac{\bar{\theta}_{1\ell}}{\bar{\theta}_{2\ell}}$ is :

$$\frac{\bar{\theta}_{1\ell}}{\bar{\theta}_{2\ell}} \propto \frac{1}{1 + \frac{s}{350}} \; \frac{1 + 2\frac{s}{540}}{1 + \frac{s}{540}} \; \frac{1 - \frac{s}{4970}}{1 + \frac{s}{4970}} \qquad \text{C1}$$

using the same technique as in Appendix B.

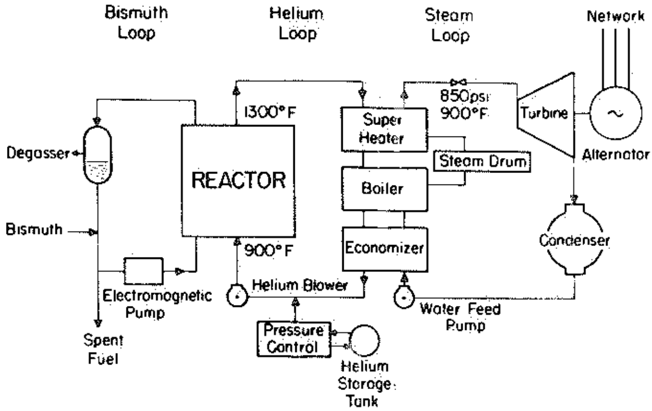

Figure 1. SIMPLIFIED PLANT DIAGRAM

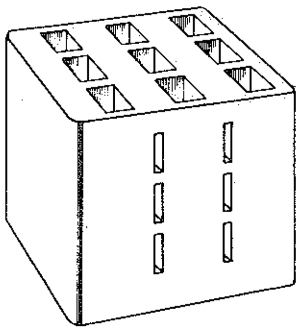

Figure 2. SECTION OF GRAPHITE CORE ELEMENT

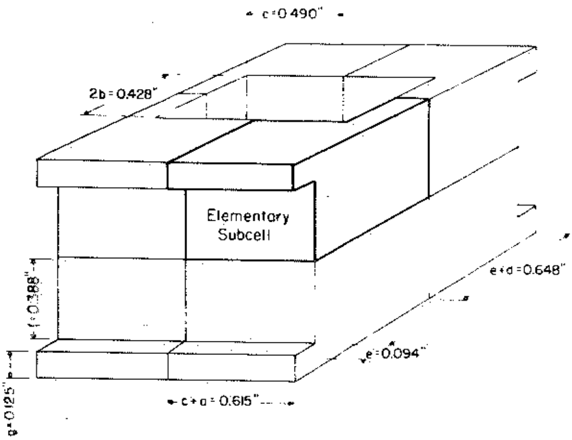

Figure 3. GRAPHITE CORE ELEMENTARY CELL

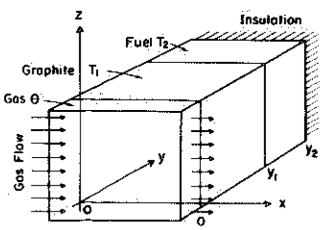

Figure 4. APPROXIMATE REACTOR CORE SUBCELL MODEL I

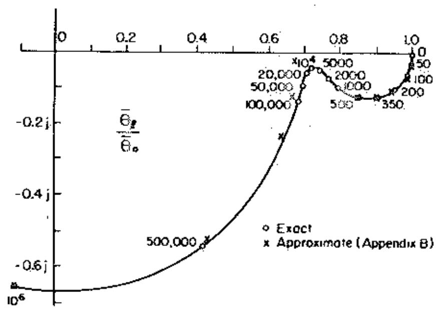

Figure 5. MODEL I - TEMPERATURE TRANSFER FUNCTION FOR $s = j\omega$

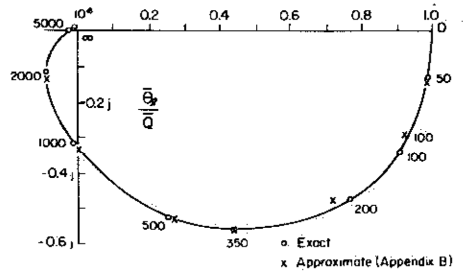

Figure 6. MODEL I - POWER TRANSFER FUNCTION FOR s = jω

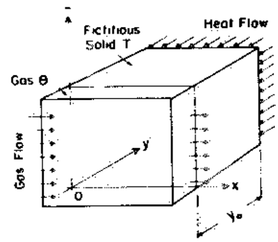

Figure 7 FICTITIOUS REACTOR CORE SUBCELL MODEL II

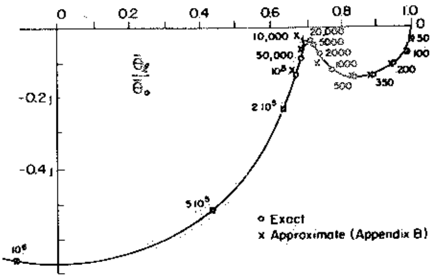

Figure 8. MODEL II - TEMPERATURE TRANSFER FUNCTION FOR s = jω

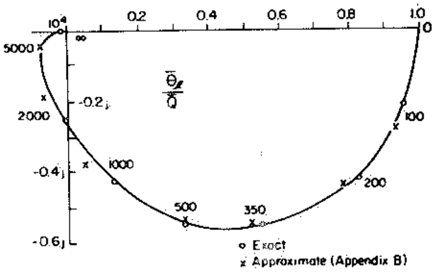

Figure 9 MODEL II - POWER TRANSFER FUNCTION FOR s = jω

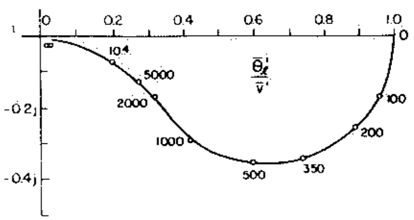

Figure 10 GAS FLOW - OUTPUT TEMPERATURE TRANSFER FUNCTION FOR s = jω

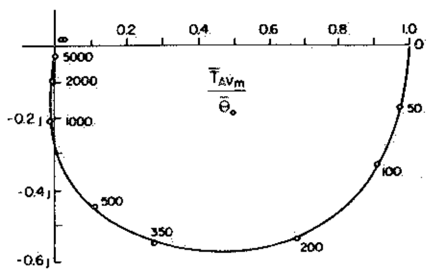

Figure 11. INPUT TEMPERATURE - MODERATOR TEMPERATURE TRANSFER FUNCTION FOR s = jω

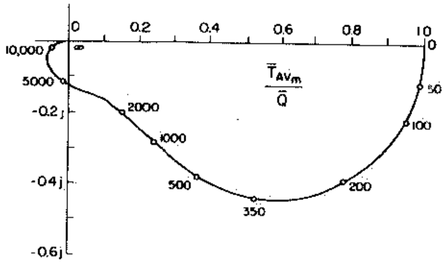

Figure 12. POWER-MODERATOR TEMPERATURE TRANSFER FUNCTION FOR s = jω

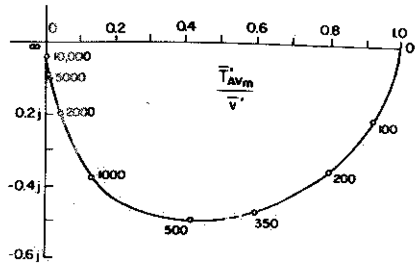

Figure 13. GAS FLOW-MODERATOR TEMPERATURE TRANSFER FUNCTION FOR s = jω

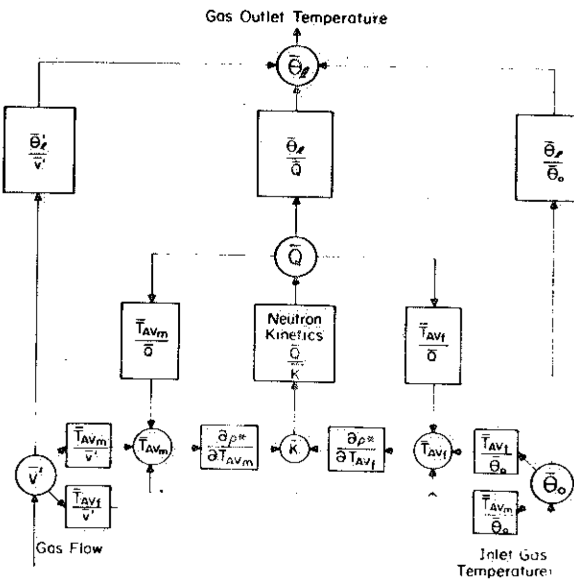

Figure 14. REACTOR BLOCK DIAGRAM

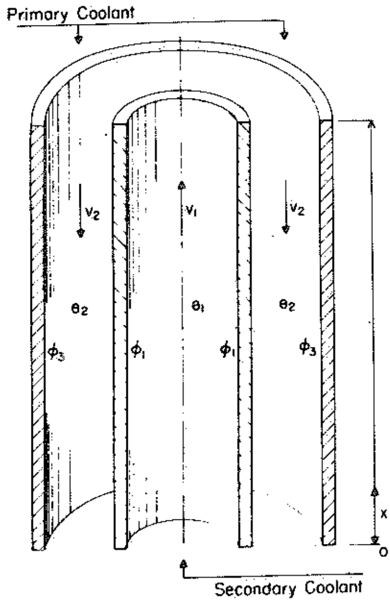

Figure 15. HEAT EXCHANGER SCHEMATIC VIEW

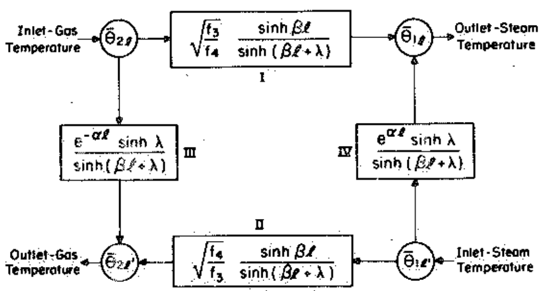

Figure 16. SUPERHEATER TRANSFER FUNCTIONS

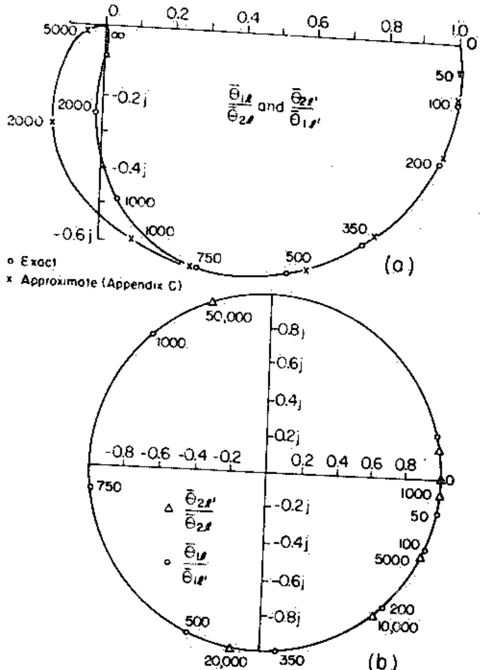

Figure 17. NORMALIZED SUPERHEATER TRANSFER FUNCTIONS FOR $s = j\omega$

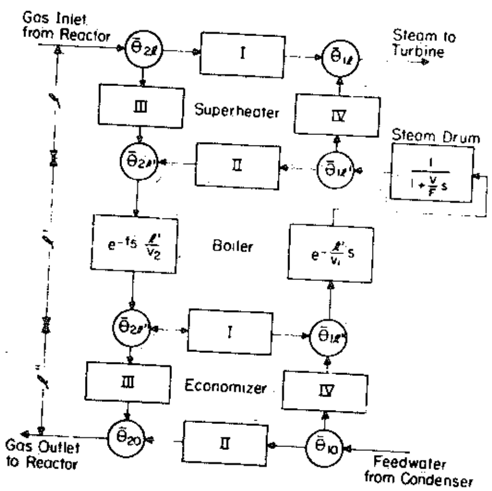

Figure 18. HEAT EXCHANGER BLOCK DIAGRAM

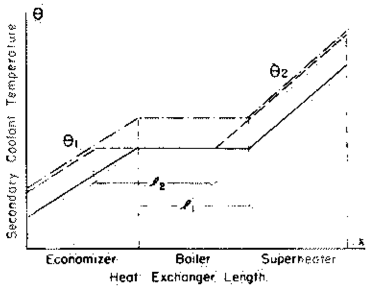

a. —— Steady state

b. ---- Actual behavior with variable feedwater temperature

c. -·- Approximation to actual behavior if $\ell_1 = \ell_2$ and $\frac{d\theta_1}{dx} = \frac{d\theta_2}{dx}$.

Figure 19. SECONDARY COOLANT TEMPERATURE ACROSS HEAT EXCHANGER

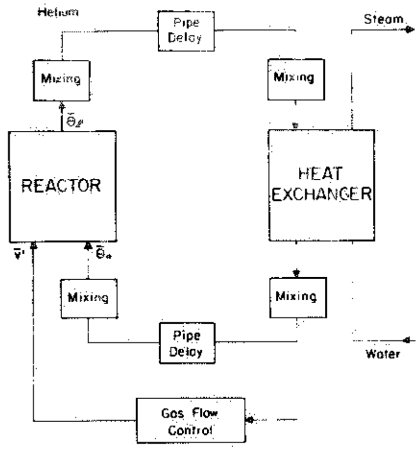

Figure 20. POWER PLANT BLOCK DIAGRAM